PROCEEDINGS of the
23rd International Congress on Acoustics
9 to 13 September 2019 in Aachen, Germany

Metaheuristic optimisation of sound absorption performance of multilayered porous materials

Vivek T. RAMAMOORTHY[(1)], Ender ÖZCAN[(1)], Andrew J. PARKES[(1)], Luc JAOUEN[(2)], François-Xavier BÉCOT[(2)]

[(1)]University of Nottingham, UK, {vivek.ramamoorthy1, ender.ozcan, andrew.parkes}@nottingham.ac.uk
[(2)]MATELYS, France, {luc.jaouen, fxb}@matelys.com

Abstract

The optimization of multilayered-sound-packaging is a challenging task which involves searching the best/optimal settings for a number of acoustic parameters. The search space size becomes too large to handle by brute force, as the number of those parameters increases. In this study, we apply metaheuristics to configure multilayered porous materials for maximizing their overall sound absorption coefficient. The multi-layered system is composed of a stack of facing screens (i.e. a woven or non-woven textile, a perforated plate) and/or thicker porous material combinations, chosen from a database of common acoustic materials. Firstly, we consider a two layered system with a fibrous porous material layer modeled using Delany-Bazley-Miki (DBM) model and a facing screen modeled by Johnson-Champoux-Allard (JCA) model, and optimize different parameters for maximizing the sound absorption. Secondly, for multilayered systems with more than two layers, a genetic algorithm is presented to explore the thickness and acoustical parameters that maximize the sound absorption coefficients for a frequency range of interest.

Keywords: Metaheuristics, Multilayered porous materials, Genetic algorithms, Sound absorption.

1 INTRODUCTION

In recent years, composite structures have been widely used in aerospace, automobile and construction applications due to their higher strength to weight ratio. Using composite construction can significantly reduce the weight and costs in these applications potentially leading to massive reductions in fuel consumption and emissions in the coming decades [1]. In automobile and aerospace composite applications, to ensure passenger comfort at similar levels as that of metallic structures, acoustic isolation design needs to be enhanced. This should be so done that the weight saving benefits are retained. Multilayered porous sound packages are commonly used to ensure noise levels are in acceptable limits. However, optimally designing these packages is a challenging task due to the large number of parameters and constraints involved, and often sub-optimal designs may be chosen for manufacture. Such problems can be tackled by using intelligent alternate metaheuristic optimisation techniques to provide near-optimal solutions in reasonable time [2]. Genetic algorithms (GA) make use of the principles of natural evolution such as, selection pressure, cross-over, and mutation to perform optimisation. After they were introduced by J. H. Holland [3] in the 1960s, they have become a widely used method for optimisation across many fields [4]. A few studies are available on the performance of metaheuristics on porous sound packaging optimisation. Tanneau et al. have used a GA for optimising transmission loss in aeronautical fuselage application [5]. Lind-Nordgren et al. [6] presented an optimisation of multilayered systems with Biot's finite element model for porous materials [7, 8, 9] by using scaling laws to link micro and macro properties. They show that the cost function landscapes have finite minima and also note that the optimisation greatly depends on the cost function. They use the method of moving asymptotes (MMA) [10] to optimise specific problem cases and have reported the optima. In this article, we give a note on the objective function landscape across different parameters of multilayered sound absorption problems modeled using a transfer matrix method (TMM) and finite-size transfer matrix method (FTMM) solver for specific absorption problem cases, and some applications of different metaheuristic techniques such as local search and GA on these problems. Successful heuristics for solving sound absorption optimisation problems could also be exploited for solving

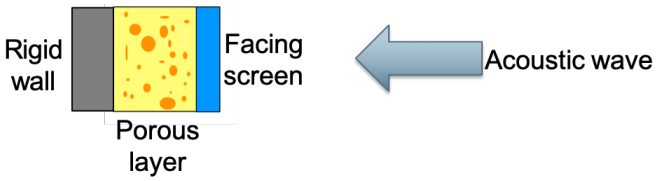


Figure 1. Two layered sound absorption system with a fibrous porous material and a facing screen.

sound transmission loss problems.

2 TWO LAYERED POROUS AND SCREEN

Consider a two layered sound absorption system with a woven or non-woven textile or a perforated plate for the first layer and a thick fibrous-porous material for the second layer backed by a rigid impervious wall as shown in the Figure 1. This type of system is commonly used in noise absorption packages. In order to efficiently optimize the acoustic performance of this two layered system, it is necessary to understand the objective function landscape before a suitable heuristic can be chosen.

2.1 Modeling the fibrous-porous layer

To model the fibrous layer, a Delany-Bazley-Miki model [11] was considered. The model describes a given porous material with the equations 1 and 2 for the characteristic impedance Z and wave number k.

$$Z = \rho_0 c_0 \left[1 + 5.50 \left(10^3 \frac{f}{\sigma_f} \right)^{-0.632} - j8.43 \left(10^3 \frac{f}{\sigma_f} \right)^{-0.632} \right] \tag{1}$$

$$k = \frac{2\pi f}{c_0} \left[1 + 7.81 \left(10^3 \frac{f}{\sigma_f} \right)^{-0.618} - j11.41 \left(10^3 \frac{f}{\sigma_f} \right)^{-0.618} \right] \tag{2}$$

In the above equations, f is the frequency in Hz, σ_f is the static airflow resistivity of the fibrous layer in $\mathrm{N{\cdot}s{\cdot}m^{-4}}$, ρ_0 is the density of air, c_0 is the speed of sound in air and $j = \sqrt{-1}$. The properties of air computed at $\mathrm{T} = 20^{\circ}\mathrm{C}$ were considered in all the following calculations. The surface impedance (Z_{M1}) at the leading face of the fibrous layer is then found for the oblique incidence scenario using equation 3.

$$Z_{M1} = \frac{-jZk}{k_3 tan(k_3 t_f)} \tag{3}$$

In the equation, t_f is the thickness of the fibrous layer and k_3 is the oblique wave number calculated from $k_3 = \sqrt{k^2 - \left(\frac{2\pi f \sin(\theta)}{c_0}\right)^2}$, where θ is the angle of oblique incidence.

2.2 Modeling the screen

We consider the procedure for modeling facing screens from [12, 13] as briefed below. TMM with the complete Johnson-Champoux-Allard model [14, 15, 16] was used to describe the fibrous porous layer. In this case, the equation 4 was used to compute the dynamic mass density of the screen ($\widetilde{\rho}_{cs}$) and the equation 5 was used to compute its dynamic bulk modulus ($\widetilde{K}_{cs}$).

$$\widetilde{\rho}_{cs}(\omega) = \frac{\alpha_\infty \rho_0}{\phi_s} \left[1 - j \frac{\sigma_s \phi_s}{\omega \rho_0 \alpha_\infty} \sqrt{1 + j \frac{4\alpha_\infty^2 \eta \rho_0 \omega}{\sigma_s^2 \Lambda_s'^2 \phi^2}} \right] \tag{4}$$

$$\widetilde{K}_{cs}(\omega) = \frac{\gamma P_0/\phi_s}{\gamma-(\gamma-1)\left[1-j\frac{8\eta}{\Lambda_s'^2 C_p \rho_0 \omega}\sqrt{1+j\frac{\Lambda_s'^2 C_p \rho_0 \omega}{16\eta}}\right]^{-1}} \tag{5}$$

Here, γ is the adiabatic index for air, P_0 is the atmospheric pressure, η is the dynamic viscosity of air, ω is the angular frequency equal to $2\pi f$, C_p is the specific heat of air at constant pressure and ϕ_s is the porosity of the screen. We compute α_∞ from the equation 6.

$$\alpha_\infty = 1+2\frac{\varepsilon}{t_s} \qquad \text{where} \qquad \varepsilon = \left(1-1.13\xi-0.09\xi^2+0.27\xi^3\right)\frac{8r}{3\pi} \qquad \text{and} \qquad \xi = 2\sqrt{\frac{\phi_s}{\pi}} \tag{6}$$

ε is the corrected length accounting for flow distortions near the screen perforations and $\Lambda_s' = r$. The value of r is computed from the relation $r = \sqrt{\frac{8\eta}{\sigma_s \phi_s}}$. Here, σ_s is the static air flow resistivity of the screen. Now, the equivalent characteristic impedance for the screen (Z_{cs}) and equivalent wave number (k_{cs}) may be computed from the relations $Z_{cs} = \sqrt{\tilde{\rho}_{cs}\widetilde{K}_{cs}}$ and $k_{cs} = \omega\sqrt{\frac{\tilde{\rho}_{cs}}{\widetilde{K}_{cs}}}$.

For the two layered system, the surface impedance Z_s can be computed from equation 7.

$$Z_s = Z_{cs}\frac{-jZ_{M1}+Z_{cs}\tan(k_{cs}t_s)}{Z_{M1}\tan(k_{cs}t_s)-jZ_{cs}} \tag{7}$$

Here, t_s is the thickness of the screen. To find the absorption, we use the formula for oblique incidence using the expression 8.

$$\alpha(\omega) = 1-\left|\frac{Z_s(\omega)-\frac{\rho_0 c_0}{sin(\theta)}}{Z_s(\omega)+\frac{\rho_0 c_0}{sin(\theta)}}\right| \tag{8}$$

2.3 Two parameter optimisation

We consider a test study where the objective function α_{rms} is maximized for different values of σ_s and σ_f while keeping the other parameters unchanged as stated in the equation 9.

$$\max_{\sigma_s,\sigma_f}\left(\alpha_{rms} = \sqrt{\frac{\Sigma_{i=1}^{N}[\alpha(f_i)]^2}{N}}\right) \tag{9}$$

For this, the thickness of the fibrous-porous layer was set to 20 mm, the thickness of the facing screen to 0.5 mm, and the porosity of the screen to 0.04 and 0.90 (in two separate cases). The absorption coefficients have been computed here for an oblique incidence of angle 34° (chosen arbitrarily for illustration purposes) for frequencies from 20 Hz to 5000 Hz in linear steps of 20 Hz. The landscape of the objective function was found to be unimodal or plateau-like in these two parameters as seen in the Figure 2. It is thus noted that a suitable local search heuristic [17] may be used for optimisation. The local search heuristics can be used solely or in conjunction with other metaheuristic methods as they exploit the neighbourhood of good solutions to improvements during optimisation.

The best α_{rms} obtained using hill climbing for fixed parameters, ϕ_s = 90%, $t_f = 20$ mm, $t_s = 0.5$ mm, at an oblique incidence angle of 34° is 0.846 and it occurs at: σ_s = 19700 N·s·m^{-4} and σ_f = 49000 N·s·m^{-4}.

2.4 Three parameter optimisation

The optimisation is extended to include the porosity of the screen ϕ_s as given in equation 10. When the objective function (α_{rms}) landscapes are plotted versus σ_f and σ_s similar to Figure 2 for various values of ϕ_s, it

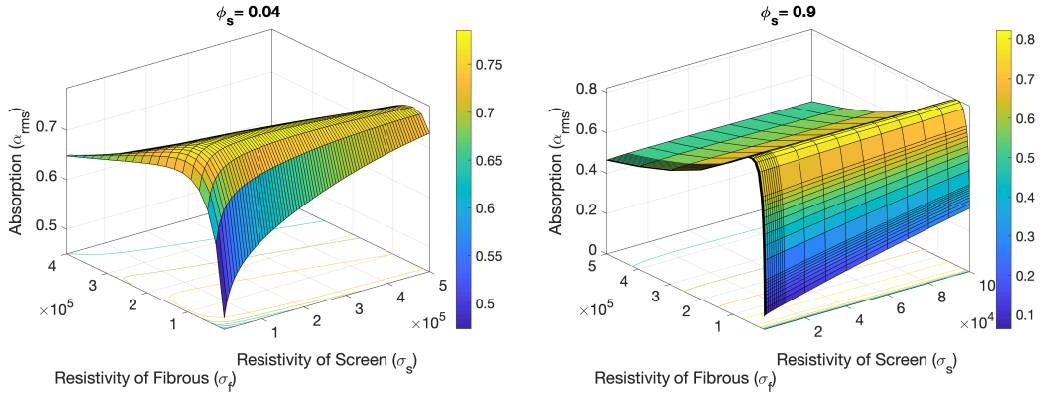


Figure 2. Absorption landscape for two layered: porous material and screen, over resistivities σ_s and σ_f for $\phi_s = 0.04$ (left) and $\phi_s = 0.90$ (right) for fixed parameters $t_f = 20$ mm, $t_s = 0.5$ mm, at an oblique incidence angle of 34°.

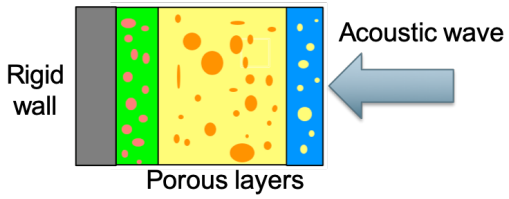


Figure 3. Three layered sound absorption system.

was observed that the landscapes grossly increased upto a certain ϕ_s, and then decrease, indicating the presence of an optimum over this parameter. Another observation was that the presense of finite modes or plateau-like nature of the landscape was retained when tuning the parameter ϕ_s.

$$\max_{\sigma_s,\sigma_f,\phi_s} \left(\alpha_{rms} = \sqrt{\frac{\Sigma_{i=1}^{N} [\alpha(f_i)]^2}{N}} \right) \tag{10}$$

For the three parameter problem, the optimum of α_{rms} occured at a porosity of the screen value of $\phi_s = 52\%$, at $\sigma_s = 1$ N·s·m^{-4} and $\sigma_f = 71100$ N·s·m^{-4} (rounded to the nearest 100). The objective function value was $\alpha_{rms} = 0.862$ at the optimum. It is noted that $\sigma_s = 1$ N·s·m^{-4} was the lower bound for that parameter in the optimisation. This means that, for the studied configuration, not using a screen is better in terms of absorption, an expected result, as the purpose of the screen is to protect the porous layer.

3 MULTI-LAYERED SOUND PACKAGE OPTIMISATION

In this section, multilayered porous packages with three or more layers are considered. For the test studies, we will ignore non-porous/impervious materials and consider only those which have open-porosities for the layers. To ensure that non physical parameter combinations are avoided, a material database of 32 common porous sound package materials is adopted. For assessing the performance of different metaheuristics in finding near optimal sound packages, we make use of the AlphaCell solver, which computes the acoustic properties for multilayered porous materials using TMM and FTMM, for evaluating the objective function.

A genetic algorithm for three or more layered sound package:
A steady state GA for the multilayered absorption problem with diffuse field is described and their results are discussed. This can be extended easily to sound transmission problems, or problems with other sound excitations (airborne or structure borne) or other phenomenological models for the system components. In a steady state GA, replacement of the offspring into the population is done after every crossover operation.

Problem Representation: Although the acoustic parameters such as thicknesses can be real valued and continuous, sub-millimetre differences in thickness neither corresponds to a significant difference in acoustic properties nor is it practical to ascertain in manufacturing the layer. Here, a discrete valued representation is proposed for thickness and other parameters, as this would reduce the search space from infinity to a finite number of configurations. As an illustration, a three layer system like shown in Figure 3 is considered with only the thickness parameters optimised while the other parameters are fixed. The chromosome (representation of a multilayered configuration) will be an array of 6 integers such as [10 6 15 20 20 20], where the first three integers represent the material choice from the database of common materials and the last three integers represent allowed discrete thicknesses or simply thicknesses in millimeters. Each combination of these 6 integers will be a different multilayered configuration. Each combination of these 6 integers will be a different multilayered configuration. The following system gives how the chromosome integers represent the material choices:

1. The material which faces the incident wave will be chosen by the first integer. This can be any material except for air and hence it can take values from 1 to $N_m - 1$, where N_m is the number of materials in the database.

2. The second material can now be air but it should not be the same as the first material. Hence, the second integer, selecting the second material, can also can take an integer value between 1 and $N_m - 1$, though now from a slightly different set.

3. Each subsequent layer can similarly have any material which is not the same as the previous layer and thus, the corresponding integers can take integer values between 1 and $N_m - 1$. This is done until the last layer.

This representation inherently avoids using the same materials in adjacent layers. For thickness parameters, the corresponding integers of the chromosome are simply used as thicknesses in millimeters.

Initialization: Initial population (group of multilayered configurations) is generated randomly using a pseudo random number generator. The seed is chosen arbitrarily but then fixed, so that the GA experiments are repeatable.

Selection: In order to enforce a selection pressure for the evolution, a tournament selection was used with a tour size of 2. To implement tournament selection, two individuals (multilayered configurations) are randomly chosen from the initial population, and the individual with better fitness is chosen as the first parent for crossover (p_1). Then, two new individuals are randomly chosen again from the initial population and the one with better fitness will be the other parent for crossover (p_2). The tournament selection is repeated in successive generations to choose parents for cross-over.

Crossover: A uniform crossover is applied to the two chosen parents from tournament selection. Every integer from the parent chromosome is flipped with a probability of 0.5. The two new chromosomes so produced will be the offspring which represent two new multilayered configurations which have characteristics from both the parent configurations.

Mutation: Mutation is performed on the offspring of crossover and a mutation probability of 1/(chromosome length) is used for each integer in the chromosome. The mutated offspring (o_1 and o_2) will then be used to evaluate the objective function which is α_{rms} using the TMM solver.

Replacement and elitism: The two mutated offspring (o_1 and o_2) from a crossover operation and the two parents (p_1 and p_2) which produced them are pooled, and the best two of these in terms of fitness (b_1 and b_2) are chosen to replace the members in the population. Two elitist schemes, strong elitism and weak elitism, are implemented and compared on the multilayered absorption problem under diffuse sound field. In strong elitism, the two best individuals from the parent-offspring pool (b_1 and b_2) will replace the two weakest members of the population (w_1 and w_2) in terms of their objective function value. Whereas, in weak elitism, the two selected individuals from the parent-offspring pool will replace the two parents (p_1 and p_2).

Results: The best fitnesses obtained from single trials of GA for strong and weak elitism were 0.887 and 0.889 respectively. But, it would not be appropriate to conclude weak elitism is better than strong elitism from this single trial. In order to compare the performance of strong and weak elitism, the evolution of average of best fitnesses across generations is plotted for 30 GA trials in Figure 4. The initial population size was 10 and the same initial random number seed was used for initializing strong and weak elitism trials essentially starting from the same initial population. We find that strong elitism in fact slightly converges faster on this problem instance. For a total thickness constraint of 60 mm, the configuration with the highest sound absorption (diffuse sound field) found from the trials, optimising only for the thicknesses and the material choice, is reported in Table 1. In the table, the layering order is from the material next to the rigid wall to the material facing the acoustic wave.

Table 1: The best configuration found for a total thickness constraint of 60 mm, with $\alpha_{rms} = 0.919$

Material	Model	t (mm)	ϕ	σ (N·s·m^{-4})	Λ (μm)	Λ' (μm)	α_∞	k_0' (10^{-10} m^2)	α_0	α_0'
Rockwool	JCAL	19	0.95	120000	12	20	1.08	10	-	-
Glasswool	JCA	23	0.99	20000	26	135	1.11	-	-	-
FoamR1	JCAPL	18	0.9	7000	129	440	1.12	83	1.22	1.13

4 CONCLUSIONS

A two layered porous and screen sound absorption system backed by a rigid impervious wall was characterized using DBM and JCA models, and the absorption performance landscape was presented. A hill climbing heuristic was applied and the optimum parameters are reported for a specific problem case. A steady state genetic algorithm based procedure was outlined for multilayer systems, using a TMM and FTMM solver to compute the acoustic indicators. An example of a three layered porous system was optimised. Also, a strong elitism seemed to converge slightly faster than weak elitism over 30 trials. On studying the landscape further over different thickness configuration for the same material configuration, the variation of the absorption performance was smooth, continuous, with finite modes and plateaus. This study will be extended further and the effectiveness of the proposed approaches will be evaluated on more complicated problems to include more layers and materials, to obtain optimal multilayered sound packaging.

ACKNOWLEDGEMENTS

This research was funded by the European Commission's Horizon 2020 research and innovation programme No2Noise under the Marie Skłodowska-Curie grant agreement no: 765472.

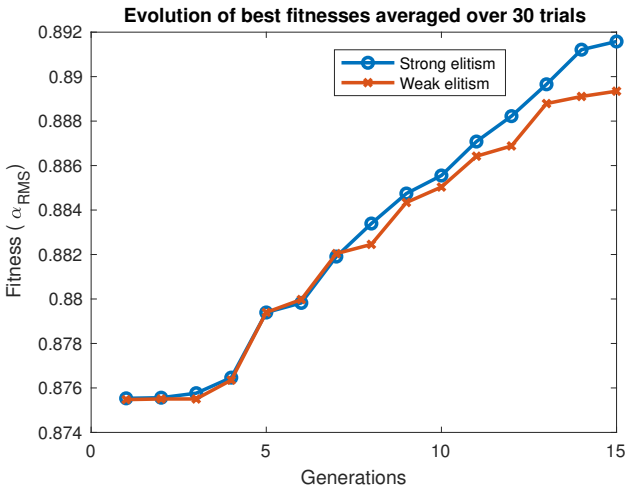


Figure 4. Comparison of average of best across 30 trials between strong and weak elitism.

References

[1] Timmis AJ, Hodzic A, Koh L, Bonner M, Soutis C, Schäfer AW, et al. Environmental impact assessment of aviation emission reduction through the implementation of composite materials. The International Journal of Life Cycle Assessment. 2015;20(2):233–243.

[2] Glover FW, Kochenberger GA. Handbook of metaheuristics. vol. 57. Springer Science & Business Media; 2006.

[3] Holland JH, et al. Adaptation in natural and artificial systems: an introductory analysis with applications to biology, control, and artificial intelligence. MIT press; 1992.

[4] Srinivas M, Patnaik LM. Genetic algorithms: A survey. computer. 1994;27(6):17–26.

[5] Tanneau O, Casimir J, Lamary P. Optimization of multilayered panels with poroelastic components for an acoustical transmission objective. The Journal of the Acoustical Society of America. 2006;120(3):1227–1238.

[6] Lind-Nordgren E, Göransson P. Optimising open porous foam for acoustical and vibrational performance. Journal of Sound and Vibration. 2010;329(7):753–767.

[7] Biot MA. Theory of elastic waves in a fluid-saturated porous solid. 1. Low frequency range. The Journal of the acoustical Society of america. 1956;28(1):168–178.

[8] Biot MA. Theory of propagation of elastic waves in a fluid-saturated porous solid. II. Higher frequency range. The Journal of the acoustical Society of america. 1956;28(2):179–191.

[9] Biot MA. Theory of deformation of a porous viscoelastic anisotropic solid. Journal of Applied Physics. 1956;27(5):459–467.

[10] Svanberg K. The method of moving asymptotes—a new method for structural optimization. International journal for numerical methods in engineering. 1987;24(2):359–373.

[11] Miki Y. Acoustical properties of porous materials-Modifications of Delany-Bazley models. Journal of the Acoustical Society of Japan (E). 1990;11(1):19–24.

[12] Atalla N, Sgard F. Modeling of perforated plates and screens using rigid frame porous models. Journal of sound and vibration. 2007;303(1-2):195–208.

[13] Jaouen L, Bécot FX. Acoustical characterization of perforated facings. The Journal of the Acoustical Society of America. 2011;129(3):1400–1406.

[14] Johnson DL, Koplik J, Dashen R. Theory of dynamic permeability and tortuosity in fluid-saturated porous media. Journal of fluid mechanics. 1987;176:379–402.

[15] Champoux Y, Allard JF. Dynamic tortuosity and bulk modulus in air-saturated porous media. Journal of applied physics. 1991;70(4):1975–1979.

[16] Brouard B, Lafarge D, Allard JF. A general method of modelling sound propagation in layered media. Journal of Sound and Vibration. 1995;183(1):129–142.

[17] Hoos HH, Stützle T. Stochastic local search: Foundations and applications. Elsevier; 2004.